# Pixel-wise Absolute Pressures in the Aortic Arch from 3D MRI Velocity Data and Carotid Artery Applanation Tonometry

Ioannis Bargiotas-*Student non-member*, Alban Redheuil, *Non-member*, Morgane Evin, *Non-member*, Alain De Cesare, *Non-member*, Emilie Bollache, *Non-member*, Gilles Soulat, *Non-member*, Elie Mousseaux, *Non-member*, Nadjia Kachenoura, *Non-member*

***Abstract*—A pixel-wise method for absolute and local aortic pressures estimation using 3D velocities in MRI and carotid pressure curves to set-up reference pressure values is presented. This method is based on the Navier-Stokes equation and a fast iterative algorithm. Its reliability was demonstrated: 1) in a synthetic phantom by comparison against simplified Bernoulli equation applied at peak velocities, and 2) in a healthy subject and a patient with aortic coarctation, in which absolute pressure distribution within the aortic arch was consistent with established physiopathological knowledge. Such local absolute aortic pressures may be useful in the understanding of hemodynamic changes secondary to cardiovascular alterations. Also, their addition to the already available indices of risk of aortic complications such as dilatation and dissection definition may prove of major clinical usefulness.**

## I. Introduction

It is now well established that aortic pressure gradients are extremely useful in characterizing diseases such as valvular stenosis and aortic coarctation [1]. Going further and estimating absolute and local pressure variations [2], at different aortic locations, would be of major usefulness for the characterization of aortic hemodynamic changes related to geometrical properties and arterial stiffness, associated with aging and aggravated by other cardiovascular risk factors [2]. Although catheterization is the gold standard for the measurement of local aortic pressures, its usefulness in clinical routine remains limited because of its invasive nature. Alternatively, applanation tonometry has been proposed for an accurate and non-invasive evaluation of pressures variations in peripheral arteries (radial, brachial, carotid, femoral, etc). Although it is well accepted that pressure distribution varies locally throughout an artery and the aorta, none of the aforementioned methods can provide the exact spatial distribution of pressures.

Since acceleration and deceleration in fluids are directly associated with pressure gradients [3],the use of spatial and temporal variations of velocities can be an alternative way for estimating pressure gradients inside an artery. In Doppler, the Bernoulli equation is often used considering maximal velocities and neglecting temporal acceleration, resulting in an estimate of pressure gradients $\Delta p = 4\times V^2_{max}$ [1]. It is widely used in characterizing pressure gradients (spatial pressure differences) in valvular stenosis, which offers an ideal situation for the application of such simplified form, since the velocity changes abruptly before, across and after the stenosis.

Recently, several studies estimated pressure gradients maps non-invasively from 2D [3], [4] in plane 3D [5] and 4D [1], [6] MRI encoding velocity data, using Navier-Stokes equations while assuming that blood is an incompressible, laminar Newtonian fluid. Other studies used MRI acceleration data directly [7], which are however not presently available on clinical MRI scanners. Methodologically, the estimation of pressure maps from MRI velocity data was based on either: 1) integrative methods along a predefined path [8] or 2) iterative methods, which estimate the local pressure as a function of neighboring pressure gradients [6]. To achieve a spatial pressure mapping using such methods, a reference point with a pressure = 0 was often used to initialize the aforementioned methods.

In this study, in-plane phase contrast (PC) MRI data with a 3D encoding of local aortic arch velocities are used to calculate absolute aortic pressure maps, throughout the cardiac cycle, using the iterative method. An original feature of our method is that instead of considering the non-realistic zero pressure reference throughout the cardiac cycle, carotid applanation tonometry pressures were used to set-up the reference pressure point, which was located at the brachial cephalic trunk on the MRI velocity images. The reliability of the resulting pressure maps was assessed on: 1) synthetic phantom data, and 2) PC-MRI aortic velocity data of a normal subject and a patient with aortic coarctation.

## II. Materials And Methods

### A. Navier-Stokes Equation

Pressure gradients ($\nabla P$) of a 3D velocity field (v) in non-turbulent Newtonian fluids can be expressed as:

$$\nabla P = -\rho(\partial v/\partial t + v\cdot\nabla v) + \mu\nabla^2 v + \rho g \qquad (1)$$

where ρ is the fluid density ($\rho_{blood}$ = 1060 kg.m$^{-3}$), μ is the dynamic viscosity ($\mu_{blood}$ = 0.0035 kg.m$^{-1}$.s$^{-1}$) and g is the gravitational force exerted on the blood. $\partial v/\partial t$ represents the temporal inertia and $v\cdot\nabla v$ the convective inertia.

I. B., A. R., M. E., A. D. C., E. B., and N. K., are with Sorbonne Universités, UPMC Univ Paris 06, CNRS 7371, INSERM 1146, Laboratoire d'Imagerie Biomédicale, F-75013, Paris, France (corresponding author I. B.: ++33-(0) 1-53-82 84 35; fax: ++33-(0) 1-53-82-84-48; e-mail: ioannisbargiotas@gmail.com).

E. M. and G. S. are with Department of Cardiovascular Radiology, Hôpital Européen Georges Pompidou, Paris, France.

A. R., M. E. are with Imaging Core Lab, ICAN, Paris, France.

I. B was co-funded through Greek State Scholarship Foundation (IKY) – academic year 2011-2012, by the funds of European Social Fund (ESF) and NSRF, 2007-2013.

### B. Phantom Data

In order to test the algorithm developed for the estimation of the pressure maps, simplified velocity phantom was designed. The phantom comprised 43 frames and two compartments in the *x* and *y* directions, with a spatially constant velocity. Temporal velocity variations were realistic, surrogating the variations of a real ascending aortic velocity. Thus, pulsatile flow curves, were placed in both compartments. To simulate velocity distribution in stenotic condition, high velocities were attributed to the second compartment and such values were divided by 4 to obtain the first compartment (Fig. 1). In addition, a Rician noise ($\sigma$=15) was added to velocity data $V_x$ and $V_y$. Finally, as shown in Fig. 2, pressure was initialized to the normal subject carotid pressure curve in the low velocity compartment.

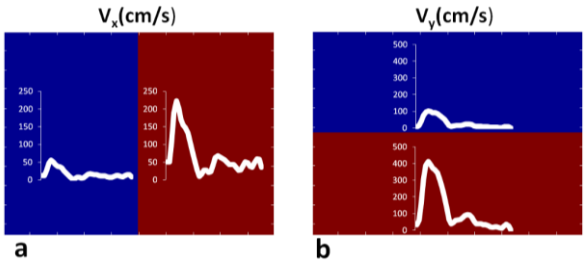


Figure 1. Phantom data with a time-varying high (red) and low (blue) velocity compartments.

### C. In Vivo Data

A healthy subject (male, 54 years old), and a patient with aortic coarctation (male, 60 years old) underwent PC-MRI and applanation tonometry. The institutional review board approved the study protocol and the two subjects signed a written consent.

MRI was performed using a 1.5T magnet (Signa HDx, GEMS, Waukesha, WI, USA) with cardiac phased-array coil and ECG-gated sequences. After localization sequences, 3D velocity were acquired in a longitudinal plane of the thoracic aorta. Scan parameters were: repetition time = 7.4 ms, echo time = 3.0 ms, flip angle = 20°, views per segment = 2, rectangular field-of-view = 50%, acquisition matrix= 256 × 256, pixel size = 1.61 mm × 1.61 mm, slice thickness = 8 mm, and encoding velocity = 200cm/s. View sharing was used resulting in an effective temporal resolution of 15 ms.

Immediately after MR acquisitions, the right carotid artery tonometry was performed with the Pulse Pen device (Diatecne, Milano, Italy). The carotid pressure curve resulted from the average of several cardiac cycles and was calculated after calibrating tonometric measurements by the brachial mean and diastolic pressures measured simultaneously to the PC-MRI acquisitions [9].

### D. Pressure Map Estimation

Algorithms and user interface were written in Matlab 2013 (The Mathworks, Natick, MA).

First, data were filtered using a 5th order digital low pass Chebyshev 1 filter, which was applied on pixels time-intensity variations of velocity data ($V_x$, $V_y$, $V_z$). Pressure gradients were estimated using the Navier-Stokes equation while neglecting gravitational forces since subjects were placed in the supine position. As previously reported, viscous resistance was also neglected [4], [5], [10]. The convective acceleration terms were estimated by the central difference formula between three consecutive pixels. Temporal acceleration was estimated using the values of two consecutive frames. Temporal acceleration was calculated in *x, y* and *z* directions while convective acceleration was estimated only in the *x* and *y* directions because of the in-plane nature of our velocity acquisitions. This resulted in pressure gradients maps which were filtered using a two dimensional 3×3 Wiener filter.

As a first step for absolute pressure maps estimation, the user draws manually a ROI within the aorta and defines a pressure reference position ($x_0$,$y_0$) at the origin of the brachial cephalic trunk. Velocity curve measured in a 3x3 neighborhood of ($x_0$,$y_0$) and carotid pressure curve were processed to account for differences in heart rate and in acquisition sites between tonometric and MRI exams. To this aim the following steps were achieved: a) setting the foot of the velocity onset to the foot of the pressure onset [9] and b) calibrating the systolic and diastolic durations independently.

Having this reference point, relative values of pressure can be estimated using integration (2):

$$P(x_1, y_1) = P(x_0, y_0) + \int_0^L \left(dp/ds\right) ds \qquad (2)$$

where $P(x_0,y_0)$ is the reference pressure value and L is the followed path line length between $(x_0,y_0)$ and $(x_1,y_1)$.

Pressure can be also estimated using iterative approach (3), as previously proposed.

$$P^{k+1} = (1-a)P^k + \frac{1}{4}a\sum_{i=1}^{4}\left(P_i^k + \nabla P_i \cdot \Delta r_i\right) \qquad (3)$$

where $P^k$ is the pressure value at the $k^{th}$ iteration, $P_i$ and $\nabla P_i$ indicates pressure and pressure gradient of the four orthogonal neighbors, $\Delta r_i$ is the distance between two consecutive pixels. The value of α was set to 0.5 as in [6][4]. The iterative algorithm ran until convergence and stopped when the relative change in the pressure was less than 0.1% between two successive iterations [1], [4], [6].

Prior to this iterative algorithm pressure maps were calculated by successively propagating the reference pressure to the nearest neighbors using the Navier-Stokes pressure gradients. First, Euclidian distance map according to the reference point was defined. Then pixels were processed according to their distance to reference and pressure of each pixel was initialized by the mean integration value of the non-zero neighborhood. This initialization is performed only when at least one of the neighboring pixels is already processed. Indeed, in C shape ROI, the distance criteria may lead to a pixel without pre-processed neighbors. Such pixels processing is therefore postponed until its neighbors are filled.

Integration and iterative methods were tested on phantom data and the most reliable was used on patients data.

## III. Results

### A. Results on Phantom Data

Fig.2 illustrates pressure curves calculated using the iterative method from noiseless $V_x$ and $V_y$. At peak velocities, pressure gradients provided by the iterative and integration methods (-15.4 mmHg for $V_x$ and -64.1 mmHg for $V_y$) were close to those found using the simplified Bernoulli equation (-16.32 mmHg and -67.3 mmHg). When rician noise was introduced in the phantom data, the pressure curve obtained from the iterative method was closer to the noiseless reference curve (0.83 mmHg) than the curve provided by the integration method while using a random pathline (4.92 mmHg). The proposed filtering of velocities and pressure gradient maps reduced these mean square errors to 0.77 and 1.40 mmHg, respectively. Dependency to pathline (Fig. 3) was demonstrated by the differences in pressure curves obtained from different pathlines (standard deviation around the mean pressure curve varied between 8.60 mmHg and 0.56 mmHg).

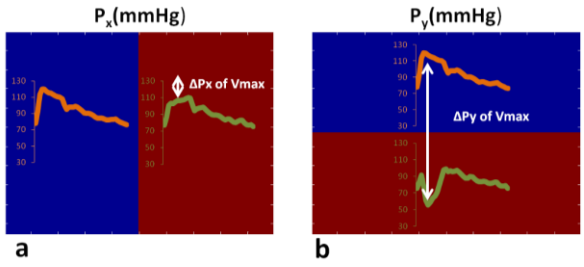


Figure 2. Phantom data with the corresponding time varying pressures. Reference pressure was placed in the low-velocity compartment (blue) and the estimated pressure curves were provided in the high velocity compartement (red). Pressure gradients corresponding to peak velocities were highlighted.

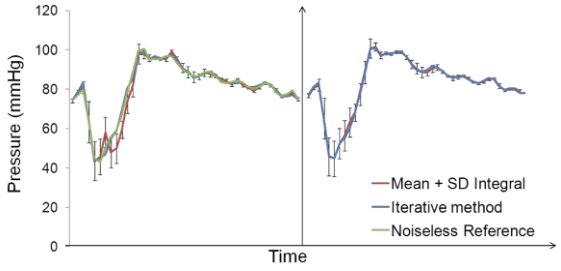


Figure 3. Pressure curves obtained in the compartement where both $V_x$ and $V_y$ were varying using integration and iterative method before (left) and after filtering (right)

### B. Results on Human Data

For each frame, depending on the ROI size, the processing time of a pressure map is around 0.5 second.

Healthy subject showed a slight increase in pressures from ascending to descending aorta in early systole and a slight decrease in late systole and early diastole. Also, an expected temporal shift between ascending and descending aortic pressure can be observed (Fig. 4).

Fig. 5 and Fig.6 illustrate respectively the aortic pressure maps obtained at four selected phases of the cardiac cycle for the healthy subject and the patient with aortic coarctation.

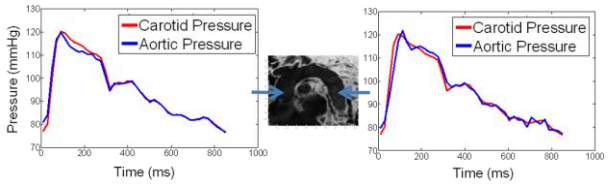


Figure 4. Carotid pressure curve (red) and ascending and descending aorta pressure curves (blue) averaged on a 5×5 region.

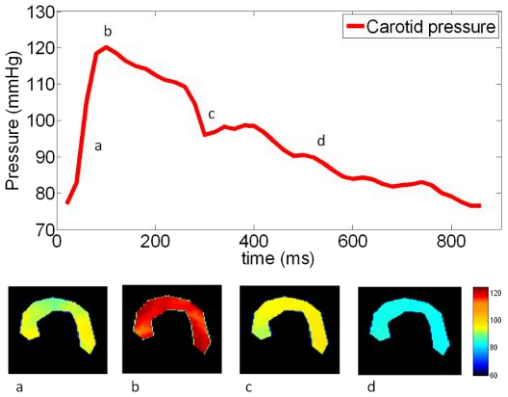


Figure 5. Pressure maps of healthy subject obtained at a) early systolic b) peak systolic c) valve closure d) middle diastolic phases defined on the carotid pressure curve.

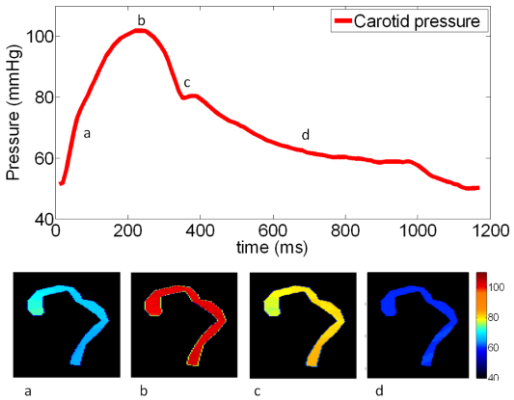


Figure 6. Pressure maps of the patient with aortic coarctation obtained at a) early systolic b) peak systolic c) valve closure d) middle diastolic phases defined on the carotid pressure curve.

For both subjects, while pressures were higher in proximal aorta in early systole, there is an increase in pressures towards periphery in late systole (Fig. 5a and Fig. 6a). The expected drop in pressure at the time of aortic valve closure was also observed on Fig. 5c and Fig. 6c. Pressure maps in the patient with aortic coarctation, indicated that pressures before the narrowing were higher than pressures

after the narrowing. Also, Fig. 6a and Fig. 6b showed the pressure recovery after the narrowing.

## IV. Discussion

In this work, the carotid pressure curve was considered as a reference for the estimation of absolute aortic pressure maps from MRI velocity data, using the Navier-Stokes equation. An iterative algorithm for a pixel-wise estimation of absolute pressure values, propagating the reference from the brachial cephalic trunk was presented. The reliability of the iterative approach was demonstrated: 1) in a bi-compartment synthetic phantom, in which good agreement was found for comparison against simplified Bernoulli equation applied in the ideal condition, and 2) in a healthy subject and a patient with aortic coarctation, in which findings were consistent with established physiopathological knowledge. Importantly, such data are obtained at the expense of only one additional short free breathing acquisition (80 sec) during the MRI exam.

Previous studies [1], [4], [6], [8] based on MRI velocity data while using similar methodological approaches to estimate relative pressures or pressure gradients have been presented in the literature. Our findings were in line with those previously presented in the literature. Indeed as in these previous studies [1], [6], the iterative approach was preferred to the integration method in our study, since integration was shown to be sensitive to the pathline [6], [8]. A drawback of these previous works is related to the choice of reference pressure location and value. Indeed, reference pressure was often positioned in the aortic valve or in the stenotic part of the aorta and was set to zero throughout the cardiac cycle. Maps of pressure variations in the healthy subject and around the aortic narrowing in the subject with coarctation were consistent with those previously reported [1]. However, a further step was achieved in our study to estimate absolute and local pressures as well as their variations throughout the cardiac cycle using a realistic boundary condition derived from the subject-specific carotid pressure curve, which was shown to be a good surrogate of aortic pressure [9]. To account for differences in acquisition site and heart-rate between MRI and applanation tonometry this pressure curve was rescaled.

As suggested in previous studies [4], [5], the Navier-Stokes viscous term was neglected in our study. Although this may cause a slight overestimation of our pressure values, its consideration may amplify the effect of noise on pressure gradients, since its estimation is given by the second order derivative of velocity data.

Since in-plane MRI velocity data were used in this study the posterior-to-anterior velocity component was not taken into account in the estimation of pressure gradients. This might induce an underestimation or an overestimation in pressure values, especially in the patient with aortic coarctation. Indeed, in this case the posterior-to-anterior velocity component is not negligible as compared to the feet-to-head and left-to-right components. To overcome this limitation, MRI 4D flow data can be used, although at the present time such data prolong considerably acquisition times (10 to 15 minutes) and generate a low temporal resolution data, which may alter the quality of the inertial component [5].

## V. Conclusion

The combination of in plane 3D MRI velocity data with carotid tonometric pressure resulted in consistent pressure maps throughout the cardiac cycle in healthy and pathological conditions. Although such results need to be confirmed on a consequent population, such estimates of absolute aortic pressure may prove its usefulness in the understanding of hemodynamic changes secondary to aging and disease. Also local pressures may be of major usefulness in optimizing the assessment of aortic complication risk with imaging, presently based only on diameter measurements, shown to be imperfect, since 50% of patients with aortic dissection have normal sized thoracic aorta[11]. Indeed, having the inner hemodynamic information in addition to changes in geometry may help for a better identification of aortic zones at risk of dissection.

## References


[1] J. Bock, A. Frydrychowicz, R. Lorenz, D. Hirtler, A. J. Barker, K. M. Johnson, R. Arnold, H. Burkhardt, J. Hennig, and M. Markl, "In vivo noninvasive 4D pressure difference mapping in the human aorta: Phantom comparison and application in healthy volunteers and patients," *Magn Reson Med*, vol. 66, no. 4, pp. 1079–1088, Oct. 2011.

[2] W. W. Nichols and M. F. O'Rourke, *Mc Donald's Blood Flow in Arteries: Theoretic, Experimental and Clinical Principles*, 6th ed. Hodder Arnold, 2011, p. 102.

[3] G.-Z. Yang, P. J. Kilner, N. B. Wood, S. R. Underwood, and D. N. Firmin, "Computation of flow pressure fields from magnetic resonance velocity mapping," *Magn Reson Med*, vol. 36, no. 4, pp. 520–526, Oct. 1996.

[4] F. Buyens, O. Jolivet, A. De Cesare, J. Bittoun, A. Herment, J.-P. Tasu, and E. Mousseaux, "Calculation of left ventricle relative pressure distribution in MRI using acceleration data," *Magn Reson Med*, vol. 53, no. 4, pp. 877–884, Apr. 2005.

[5] R. B. Thompson and E. R. McVeigh, "Fast measurement of intracardiac pressure differences with 2D breath-hold phase-contrast MRI," *Magn Reson Med*, vol. 49, no. 6, pp. 1056–1066, Jun. 2003.

[6] J. M. Tyszka, D. H. Laidlaw, J. W. Asa, and J. M. Silverman, "Three-dimensional, time-resolved (4D) relative pressure mapping using magnetic resonance imaging," *J Magn Reson Imaging*, vol. 12, no. 2, pp. 321–329, Aug. 2000.

[7] F. Balleux-Buyens, O. Jolivet, J. Bittoun, and A. Herment, "Velocity encoding versus acceleration encoding for pressure gradient estimation in MR haemodynamic studies," *Phys Med Biol*, vol. 51, no. 19, p. 4747, 2006.

[8] T. Ebbers, L. Wigström, A. F. Bolger, J. Engvall, and M. Karlsson, "Estimation of relative cardiovascular pressures using time-resolved three-dimensional phase contrast MRI," *Magn Reson Med*, vol. 45, no. 5, pp. 872–879, May 2001.

[9] S. Laurent, J. Cockcroft, L. Van Bortel, P. Boutouyrie, C. Giannattasio, D. Hayoz, B. Pannier, C. Vlachopoulos, I. Wilkinson, and H. Struijker-Boudier, "Expert consensus document on arterial stiffness: methodological issues and clinical applications," *Eur Hear J* , vol. 27 , no. 21 , pp. 2588–2605, Nov. 2006.

[10] T. Ebbers and G. Farnebäck, "Improving computation of cardiovascular relative pressure fields from velocity MRI," *J Magn Reson Imaging*, vol. 30, no. 1, pp. 54–61, Jul. 2009.

[11] J. A. Elefteriades and E. A. Farkas, "Thoracic Aortic Aneurysm: Clinically Pertinent Controversies and Uncertainties," *J Am Coll Cardiol*, vol. 55, no. 9, pp. 841–857, Mar. 2010.